4-26-2023

Characterization of Extended Uncertainty Principle Black Holes

Juan Uribe
juribe9@lion.lmu.edu

Jonas Mureika
Loyola Marymount University, jonas.mureika@lmu.edu

Loyola Marymount University
University Honors Program

CHARACTERIZATION OF EXTENDED UNCERTAINTY PRINCIPLE BLACK HOLES

A thesis submitted in partial satisfaction

of the requirements of the University Honors Program

of Loyola Marymount University

by

Juan Uribe

05/02/2023

CHARACTERIZATION OF EXTENDED UNCERTAINTY PRINCIPLE BLACK HOLES

by

Juan Uribe

A senior thesis submitted to the faculty of
Loyola Marymount University
in partial fulfilment of the requirements for the degree of

Bachelor of Science

Department of Physics

Loyola Marymount University

April 2023

THESIS COMMITTEE APPROVAL

of a thesis submitted by

Juan Uribe

This thesis has been read by each member of the following thesis committee and by majority vote has been found to be satisfactory.

02 May 2023 — Date

Dr. Jonas Mureika, Advisor and Thesis Coordinator

02 May 2023 — Date

Dr. David Berube

2 May 2023 — Date

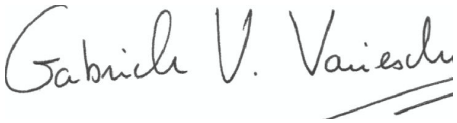

Dr. Gabriele Varieschi

ABSTRACT

Black Holes are special objects as they are at the intersection of Quantum Mechanics and General Relativity. A central tenant of quantum mechanics is the Uncertainty Principle that dictates we cannot know with complete certainty position and momentum at the same time. The Extended Uncertainty Principle introduces a position-related uncertainty correction L_* to account for General Relativity. In a previous paper, a black hole metric associated with the Extended Uncertainty Principle was derived, by modifying the metric function of a Schwarzschild black hole. This metric introduces near-horizon structures that should produce observable effects, such as love numbers, gravitational wave echoes, quasi-normal modes, and absorption coefficients. Some of these effects could be observed with current or near-term technology such as the Laser Interferometer Gravitational Wave Observatory (LIGO) and the Event Horizon Telescope (EHT). Other than calculating the expected value of the aforementioned observables, this article discusses the magnitude of L_*.

CONTENTS

ACKNOWLEDGEMENTS

Quiero comenzar agradeciendo a mi familia, a mi papá Carlos, mi mama Diana, y mi hermana María por ayudarme llegar a este punto, apoyarme, y creer en mí y mi futuro.

I also want to thank Lauren for being my support, Jimmy for being there since freshman year, and every other one of my friends that helped me get through these 4 years.

Finally, I want to thank my thesis advisor Dr. Jonas Mureika for his mentorship during this project, Dr. David Berube for his help in making my major a reality, and every other professor that helped me get here.

CHAPTER 1: INTRODUCTION

During the 20th century, two of the most prominent theories in physics arose. On one hand, quantum mechanics was formulated to explain intermolecular forces, electromagnetism, and subatomic particles. On the other hand, general relativity explained gravitational phenomena and the behavior of massive objects. These theories have dominated the field for a century and have proved to be correct on many occasions. General Relativity in relation to gravity and massive objects, and quantum mechanics in relation to all other forces and subatomic scales. However, these theories are not compatible and as such we have to look for new ones. The study of black holes is a great place to start since they are at the intersection of these two theories.

1.1 Black Holes and General Relativity

Around the same time quantum mechanics was being formulated, Albert Einstein was proposing General Relativity. In his theory, he proposed that instead of gravity acting through a field produced by mass, gravity curves the fabric of space-time around mass. In other words, gravity does not change the path that the object is traveling but it changes the structure of the path itself. To formalize this idea he derived what are now called Einstein's equations:

$$R_{\mu\nu} - \frac{1}{2}Rg_{\mu\nu} + \Lambda g_{\mu\nu} = \frac{8\pi G}{c^4}T_{\mu\nu} \tag{1.1.1}$$

where $R_{\mu\nu}$ is the Ricci tensor, R is the Ricci scalar, $g_{\mu\nu}$ is the metric, Λ is the cosmological constant, G is Newton's universal law of gravitation, and $T_{\mu\nu}$ is the stress-energy tensor. For more information on these quantities, their derivation, and/or physical meaning readers can refer to [1].

The objective of Equation 1.1.1 is to derive a metric ($g_{\mu\nu}$) given the stress-energy tensor of space (the mass and energy distribution). This quantity can completely describe the geometry of space-time by defining the line element, and as such show how gravity acts in a given space. The line element is obtained as:

$$ds^2 = g_{\mu\nu} dx^\mu dx^\nu \tag{1.1.2}$$

where x is the four-position vector.

The first solution to Equation 1.1.1 came about in 1916 by Karl Schwarzschild [2]. He derived a metric for a space-time that is asymptotically flat and has a spherically-symmetric static mass (M) in the center,

$$ds^2 = \left(1 - \frac{2GM}{c^2 r}\right) dt^2 - \frac{dr^2}{1 - \frac{2GM}{c^2 r}} - r^2 d\Omega^2 \tag{1.1.3}$$

The full derivation of this metric can be found in [3].

The components g_{tt} and g_{rr}^{-1} are what is defined as the metric function ($f(r)$) in a Schwarzschild solution.

$$f(r) = 1 - \frac{2GM}{c^2 r} \tag{1.1.4}$$

If we analyze Equation 1.1.3 we observe that when r or $f(r)$ go to 0 we have an indeterminate expression. On one hand, when r goes to 0, g_{tt} is indeterminate and we have a singularity—a location where the curvature of space-time is infinite. On the other hand, when $f(r)$ goes to 0, g_{rr} is indeterminate and we have a horizon. This horizon is the radius of a Black Hole—an object that is so dense that it has a gravitational pull that not even light can escape. The specific point of no return is called the horizon and happens when

$$r = \frac{2GM}{c^2} = R_s \tag{1.1.5}$$

This is called the Schwarzschild radius. However, this is not a true singularity, since it can be removed by choosing a different set of coordinates [4]. Equation 1.1.5 also shows that the radius of a black hole only depends on its mass. In general, most quantities of Schwarzschild-like black holes will only depend on the mass, since they do not rotate or have a charge.

1.2 Uncertainty Principles and Quantum Mechanics

In the early 20th century, it was discovered that particles possessed wave-like properties. As such, quantum mechanics describes particles using wave functions, instead of the classical-mechanical quantities. To work with these new objects, the idea of linear operators was introduced. The classical quantities were converted into operators that could help us describe the particle-like characteristics of these waves. However, operators do not behave as scalar quantities. One of the main differences is that operators do not necessarily commute—meaning that $\hat{A}\hat{B} - \hat{B}\hat{A}$ can have a non-zero value. This expression is defined as the commutator of $\hat{A}$ and $\hat{B}$:

$$[\hat{A}, \hat{B}] = \hat{A}\hat{B} - \hat{B}\hat{A} \tag{1.2.6}$$

As mentioned before, classical-mechanical quantities become operators in quantum mechanics. As such, both position and momentum became operators and we can calculate their commutator (which in the past would have been 0):

$$[\hat{X}, \hat{P}] = i \tag{1.2.7}$$

(we use $\hbar = 1$ throughout the paper).

One can use this principle to derive Heisenberg's Uncertainty principle (HUP)

$$\Delta x \Delta p \gtrsim 1 \tag{1.2.8}$$

This principle establishes that the uncertainty in position times the uncertainty in momentum has to always be greater than 1. Therefore, we are never able to make a measure with complete certainty in either of these quantities.

In the original 1927 paper [5], Heisenberg derived this principle from the quantization of the momentum of a photon. However, as shown in [6] these two approaches are equivalent.

This principle is derived without taking into account any gravitational effects. It is a purely quantum mechanical result. If we decide to consider these effects, then we can derive a modification to the HUP

$$\Delta x \Delta p \gtrsim 1 + \beta l_p^2 \Delta p^2 \tag{1.2.9}$$

This inequality is referred to as the Generalized Uncertainty Principle (GUP), where β is a positive dimensionless parameter, and l_p is the Planck length [7–9].

By doing this modification, one loses the initial symmetry of the HUP. The symmetry can be restored, by adding a Δx^2 term on the right-hand side

$$\Delta x \Delta p \gtrsim 1 + \beta l_p^2 \Delta p^2 + \alpha \frac{\Delta x^2}{L_*} \tag{1.2.10}$$

where α is a dimensionless constant of order unitary and L_* is a new large fundamental distance scale [8–11]. This is known as the Generalized Extended Uncertainty Principle (GEUP). If we ignore the Δp^2 then, we refer to it as the Extended Uncertainty

Principle (EUP)

$$\Delta x \Delta p \gtrsim 1 + \alpha \frac{\Delta x^2}{L_*} \tag{1.2.11}$$

As shown in [9], this equation can also be derived from gravitational considerations as done with the GUP. The main difference between these two is that we can observe the effects of the former over short distances, while the effects of the latter are only observable at very large distance scales [9]. Constraints on L_* will be further discussed in section 2.1.

1.3 Quantum Gravity

The last two sections have focused on the two main Physics theories of the 20th century. Both theories have been proven to be correct multiple times by observational evidence. Nevertheless, there is a problem: both theories cannot be completely correct if the other one is. Therefore, in recent years, we have been trying to come up with a theory that unifies both fields. This would be a theory for quantum gravity. We have many of them, such as loop quantum gravity [12], string theory [13], and non-commutative geometry [14]. The problem is that to find which one is correct we would have to be able to probe gravity in the quantum domain, which at this point is not possible. An alternative to this is to analyze objects that have strong gravitational fields but are subject to quantum effects. Black holes are such objects. Therefore, by better understanding black holes we are able to understand the nature of quantum gravity.

In recent years, we have made advances in technology that let us probe the nature of black holes. The two main ones are the Laser Interferometer Gravitational Wave Observatory (LIGO)[15] and the Event Horizon Telescope (EHT)[16]. On one hand, in 2015 LIGO was able to identify for the first time gravitational waves produced

by a Binary Black Hole (BBH) merger[17]. Since then it has detected almost 100 gravitational waves from different binary systems. On the other hand, the EHT was able to observe a black hole (M87*) for the first time ever in 2018 [18].

These technologies are allowing us to test the nature of black holes, and as such test theories that combine quantum mechanics and gravitation. One of these theories is EUP gravitation. If this is actually in play, then supermassive black holes (SMBHs) and the EHT provide the best chance for observationally testing this hypothesis. Therefore, we will be examining black holes under a Schwarzschild EUP-modified metric. Specifically, we will be exploring possible values for the observables of such objects and proposing limits for L_*.

CHAPTER 2: RELATED WORK

2.1 EUP metric

In section 1.1 we introduced the Schwarzschild metric and in section section 1.2 we introduced the EUP. In [11] the author proposes a derivation that brings these two ideas together to get a EUP-inspired metric. This derivation starts by suggesting that the position uncertainty (Δx) for every graviton inside the black hole is given by the Schwarzschild radius (R_s) since the graviton is inside the BH and this is its size. In other words $\Delta x = R_s$. Additionally, we set $\Delta p = p$ since the uncertainty in p is going to be the momentum of such gravitons inside the black hole. Therefore, based on Equation 1.2.11 we get:

$$p \sim \frac{1}{R_S}\left(1 + \frac{\alpha R_s^2}{L_*^2}\right) \tag{2.1.1}$$

Additionally, the number of gravitons inside a BH is given by $N_g = M_{BH}R_s$ [19], and the Schwarzschild radius is given by Equation 1.1.5

$$pN_g \sim M_{BH}\left(1 + \frac{4\alpha G^2 M^2}{c^4 L_*^2}\right) \tag{2.1.2}$$

For BHs where $R_s \ll L_*$, pN_g is just equal to the ADM mass of the black hole,

$$M_{ADM} = M\left(1 + \frac{4\alpha G^2 M^2}{c^4 L_*^2}\right) \tag{2.1.3}$$

the ADM mass is the mass as measured by an observer at infinity.

Finally, we can substitute the mass term in the Schwarzschild metric function (Equa-

tion 1.1.4) with the ADM mass

$$f(r) = 1 - \frac{2GM}{c^2 r}\left(1 + \frac{4\alpha G^2 M^2}{c^4 L_*^2}\right) \tag{2.1.4}$$

We can additionally define

$$\epsilon \equiv \frac{4\alpha G^2 M^2}{c^4 L_*^2} \tag{2.1.5}$$

and simplify the metric function as

$$f(r) = 1 - \frac{2GM}{c^2 r}(1 + \epsilon) \tag{2.1.6}$$

This equation shows that for values where $\epsilon \ll 1$ we actually recuperate the original Schwarzschild metric. This is important since we know that the Schwarzschild metric works on smaller scales so we would like to keep this behavior in the new metric, and only introduce deviations for larger objects.

Additionally, The value of L_* has not been fully determined yet but it does have some constraints. Experimental data in [11] defines a lower bound of 10^{12} m. The maximum mass of a black hole is given when the horizon radius is the Hubble length. This means that there is also a maximum possible mass. When using this framework, the maximum mass is given by

$$M_{max} \sim \frac{c^2 (L_H L_*^2)^{1/3}}{2G} \tag{2.1.7}$$

However, the value of M_{max} for $L_* < 10^{12}$ can be ruled out by observational data, according to [11].

For more information on this derivation or the theory behind it, please refer to [11].

2.2 GUP stars

In the paper [20], the authors derived a metric similar to the one in the previous chapter, but instead of using the EUP they focused their research on the GUP and BHs (Equation 1.2.9). In their paper, they derived a metric of the same form as Equation 2.1.6 but where ϵ was defined as:

$$\epsilon \equiv \gamma + \frac{1}{4}\frac{M_p^2}{M^2} \tag{2.2.8}$$

where $\gamma = \beta - 1$ and M_p is the Planck mass.

In this paper, they proposed the idea that because of the inclusion of QM in the metric function of the Black Hole, we can not consider these objects really black. Instead, they will have a near-horizon structure that will produce observable effects that will depend on the mass of the BH and the value of γ. They analyzed gravitational wave echoes, quasi-normal modes, and tidal love numbers [20]. All of these quantities will be explained in the following chapter.

CHAPTER 3: CALCULATIONS AND RESULTS

In this chapter, we will be calculating the values for observable quantities of the EUP BHs described by Equation 2.1.4.

3.1 Gravitational Wave Echoes

After a BH merger, Gravitational Waves (GWs) are created and radiated by the BH. In this case, these GWs or other incoming ones can get trapped between the two points of highest potential: the near-horizon structure at $\frac{2GM}{c^2}(1+\epsilon)$ and the photon sphere located at $\frac{3GM}{c^2}$ [20–22]. These two high potential surfaces create an echo chamber for the GWs, where the incoming waves bounce off the near-horizon structure, and then part of them bounce off the photon sphere back to the surface, and some other leave the photon sphere towards the space-like infinity (refer to Figure 3.1) [20–22].

However, the near-horizon structure is growing as M^3 while the photon sphere is only growing as M, and a photon sphere is required for the echoes to be produced. This condition imposes a limit for ϵ such that $\epsilon < 0.5$ [20]. This limit on ϵ also establishes a limit on the relationship between M and L_*:

$$\frac{M}{M_\odot} < L_* \times 10^{-4} \tag{3.1.1}$$

This upper limit represents the moment where both the near-horizon structure and the photon sphere are located at the same location and therefore there is no longer an echo chamber. At the same time, this means that there is a range of BHs for a given value of L_* that won't produce any echoes as shown in Figure 3.2. This graph also shows that for the range of values of L_* the maximum mass that produces an

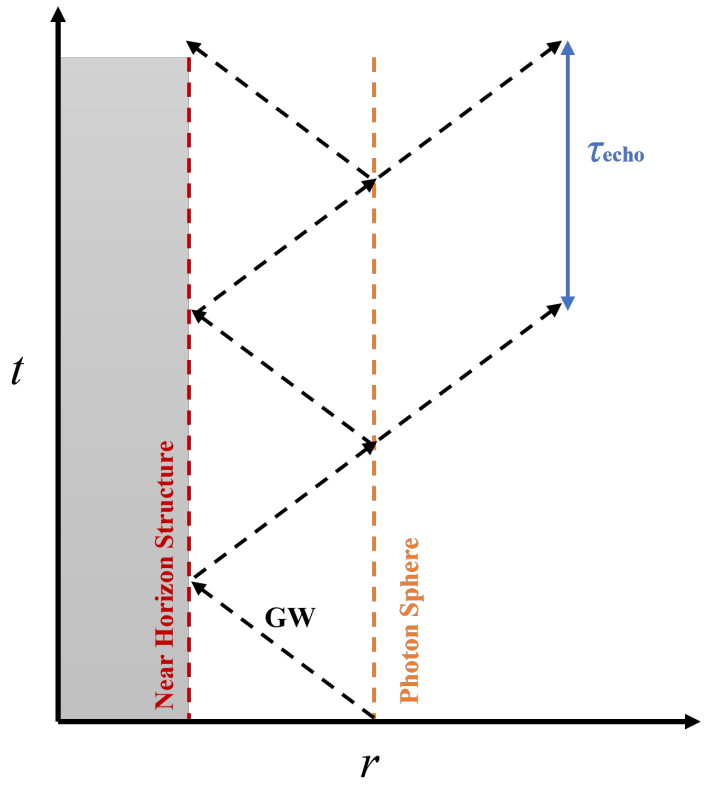

Figure 3.1: Spacetime depiction of gravitational wave echoes from the near-horizon structure introduced by the EUP located at $\frac{2GM}{c^2}(1+\epsilon)$ and the Photon Sphere located at $\frac{3GM}{c^2}$. Adapted from [21] and [22].

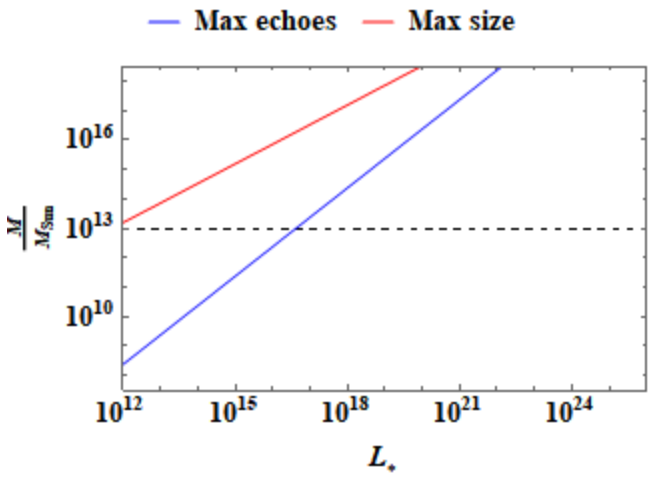

Figure 3.2: Maximum mass of BHs as a function of L_*. The blue line represents the maximum mass for a BH to produce GW echoes (Equation 3.1.1) and the red line shows the maximum size for a BH (Equation 2.1.7). The blasck dashed line represents the theoretical maximum mass for a black hole.

echo is always lower than the maximum theoretical size given by Equation 2.1.7.

As shown in Figure 3.1 the most important quantity to characterize the echoes is their period (τ_{echo}) since it is constant. This fundamental time can be calculated (as shown in [20; 21; 23], this quantity is given by

$$\begin{aligned}\tau_{echo} &= 2\int_{\frac{2GM}{c^2}(1+\epsilon)}^{\frac{3GM}{c^2}} \frac{dr}{f(r)} \\ &= \frac{2GM}{c^3}(1-2\epsilon-2\log(2\epsilon))\end{aligned} \tag{3.1.2}$$

If we replace ϵ with Equation 2.1.5 we get

$$\tau_{echo} = \frac{2GM}{c^3}\left(1-\frac{8\alpha G^2M^2}{c^4L_*^2}-2\log\left(\frac{8\alpha G^2M^2}{c^4L_*^2}\right)\right) \tag{3.1.3}$$

We can calculate the period for BHs of different masses given multiple values of L_* as shown in Figure 3.3. As seen in the figure, for smaller values of L_* the cut-off for which

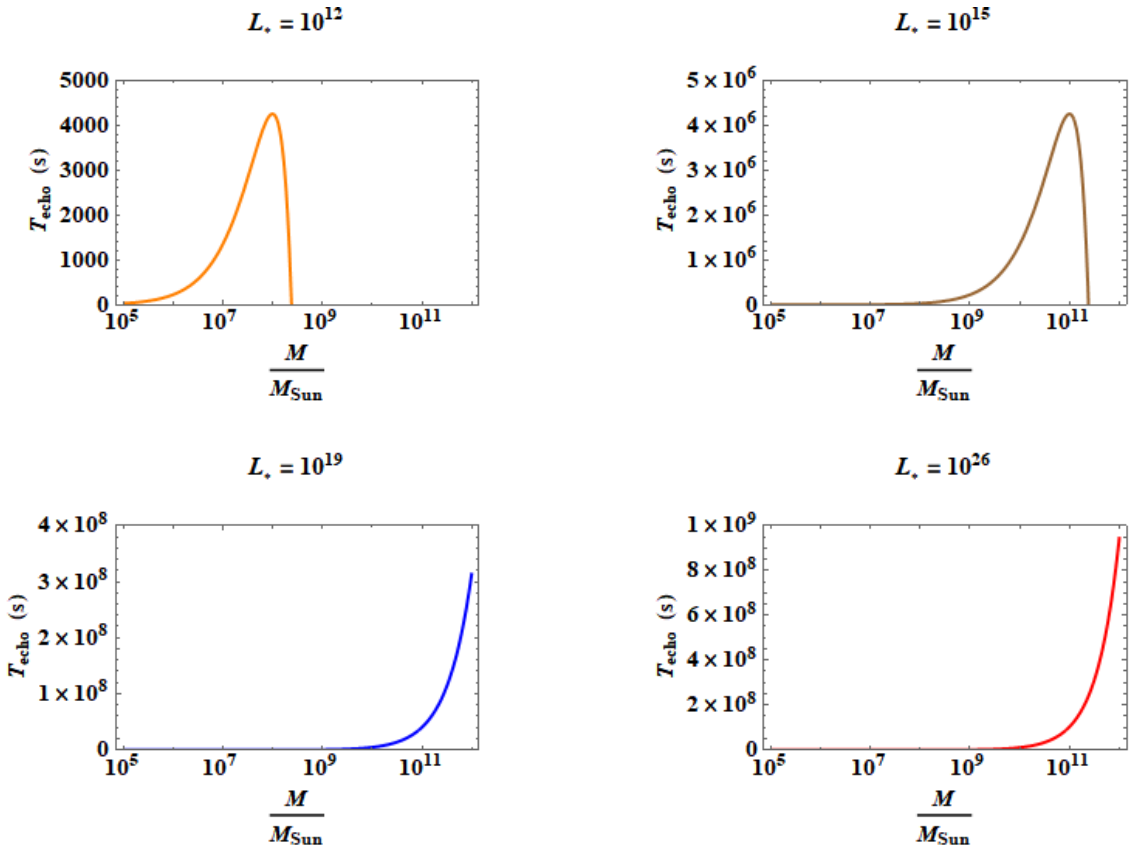

Figure 3.3: Echoes periods in seconds as a function of the mass of the black hole for four different values of L_*.

BHs can generate echoes is at a mass smaller than the theoretically largest BHs of mass around $10^{11} M_\odot$. Additionally, the maximum period increases significantly with the increase of L_*.

Figure 3.4 shows better the relation between the periods for the four values of L_* shown in Figure 3.3. In this figure, it is clear that if we were able to identify certain values for the periods we would be able to constrain the value of L_* significantly. Additionally, if we also had the mass of the BH we would be able to almost completely determine the value of this constant.

Another interesting element about Figure 3.3 and Figure 3.4 is the existence of this maximum echo produced and the subsequent downturn. This maximum is found at $\epsilon \sim \frac{1}{12}$.

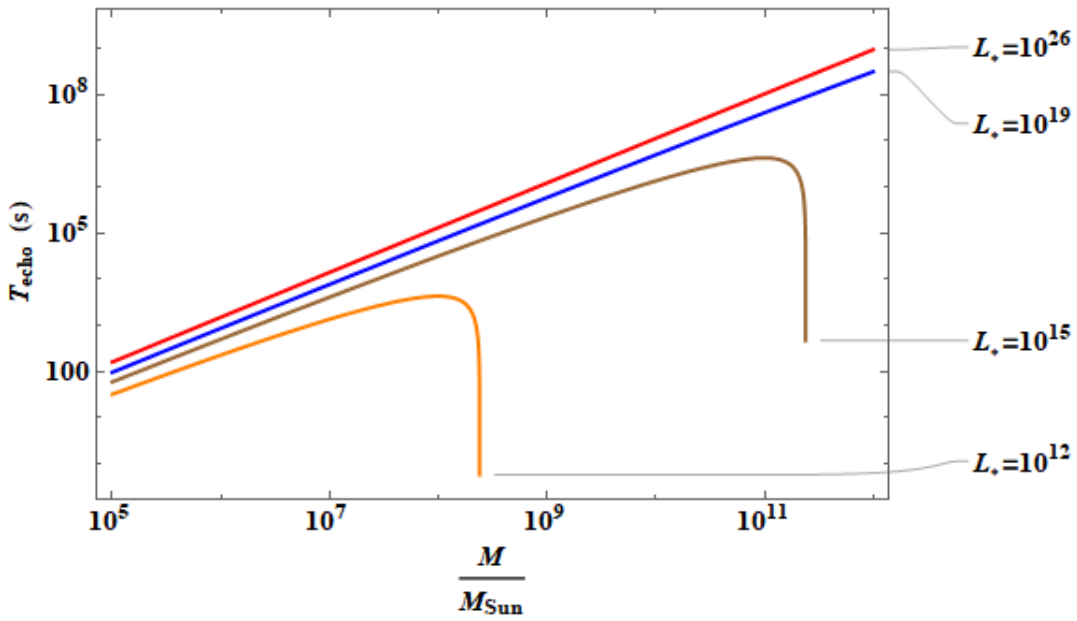

Figure 3.4: The four graphs of Figure 3.3 in one Log-Log plot.

3.2 Quasi-Normal Modes

Quasi-Normal Modes refer to perturbations on the Black Hole metric, introduced by outgoing gravitational waves [21; 24; 25]. This value is described by a real and an imaginary component [20; 25] where the former is the actual frequency of oscillation and the latter the dampening [25].

These modes of oscillation can be calculated by solving

$$\frac{\partial^2\Psi(t,z)}{\partial z^2} - \frac{\partial^2\Psi(t,z)}{\partial t^2} - V(r)\Psi(t,z) = S(t,z) \tag{3.2.4}$$

where the metric fluctuations are encoded in Ψ, V represents the potential and S is the cause of the perturbations [21]. According to [20; 21], Equation 3.2.4 can be simplified when written in Fourier space as

$$\frac{d^2\Psi(z)}{dz^2} + [\omega^2 - V(r(z))] = 0 \tag{3.2.5}$$

where ω is the complex frequency mentioned at the beginning that has a real component ω_R and the imaginary ω_I. Solving this equation for the exact values of the frequency is beyond the scope of this research, but [20; 21], presents the solution for when there is a perturbation to the Schwarzschild metric ϵ and $\epsilon \ll 1$. The approximate solution for the real component is

$$\frac{GM}{c^3}\omega_R \sim |\log \epsilon|^{-1} = \left|\log\left(\frac{4\alpha G^2 M^2}{c^4 L_*^2}\right)\right|^{-1} \tag{3.2.6}$$

and the imaginary component is

$$\frac{GM}{c^3}\omega_I \sim -\omega_R^{2l+3} = -\left|\log\left(\frac{4\alpha G^2 M^2}{c^4 L_*^2}\right)\right|^{-(2l+3)} \tag{3.2.7}$$

where l is the quantized angular momentum that is greater than the spin s of the perturbation [20].

The analysis of Equation 3.2.7 is outside of the scope of this research, but Equation 3.2.6 has been plotted for a range of masses given three possible values of L_* in Figure 3.5.

Additionally, it is possible to approximate the QNMs of a Schwarzchild BH by modifying the potential [26]. In this case, the approximation yields a frequency of

$$\frac{GM}{c^3}\omega = 0.1148 - 0.1148i \tag{3.2.8}$$

The real component of this frequency is plotted in Figure 3.5 alongside the three other values of L_*. This graph clearly shows the inverse relationship between the mass of

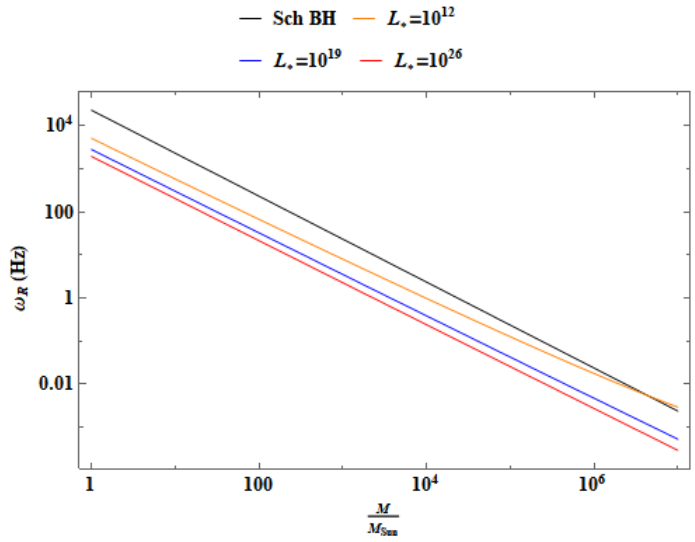

Figure 3.5: Real frequency of the quasi-normal modes for black holes of different masses given three possible values of L_*. Additionally, the exact solution for the Schwarzchild solution found in [26] is plotted in black.

the black hole and the frequency oscillation. Additionally, lower values of L_* produce higher frequencies, meaning that the measurement of QNMs should provide a clear test for this theory.

3.3 Tidal Love Numbers

Tidal Love Numbers (TDLs) parameterize the tidal deformability of an object surrounded by a tidal environment of gravitational waves [27]. This environment is found in a binary system of BHs that are spinning around each other causing a significant amount of strong gravitational waves [20; 21; 27].

The process to exactly calculating these values can be found in [27] but this article will be using the analytic estimation [20; 21] that applies when $\epsilon \ll 1$

$$k \sim |\log \epsilon|^{-1} = \left|\log\left(\frac{4\alpha G^2 M^2}{c^4 L_*^2}\right)\right|^{-1} \tag{3.3.9}$$

We can solve Equation 3.3.9 for L_* to understand the dependence between mass and k on the possible values of L_*

$$L_* \sim \sqrt{\alpha}\frac{2GM}{c^2}e^{\pm\frac{1}{2k}} \tag{3.3.10}$$

With current LISA technology, we are able to determine values of up to $k \sim 0.02$, which imposes the limit $k > 0.02$ and therefore based on Equation 3.3.10 we can impose the limit of measurable values of L_*

$$L_* > \sqrt{\alpha}\frac{2GM}{c^2}e^{\frac{1}{2*0.02}} \sim 10^{-17}M \tag{3.3.11}$$

This relationship shows that we will only be able to impose a lower limit on L_* and possibly determine its value as long as the mass of the black hole is 17 orders of magnitude smaller than L_*.

We can go even further and plot Equation 3.3.10 for different TLNs as shown in Figure 3.6.

This figure shows that the range of values that we can detect for L_* is reduced as we increase the mass of the BH, which means that measuring this value for smaller BHs will give us the best insight into this theory. Additionally, LISA is supposed to able able to measure values of up to 0.005 in the near future [20]. However, if this theory is correct, we should not expect to be able to measure this value since in Figure 3.6 the line for $k \sim 0.005$ is above the maximum theoretical value of 10^{26}. Also, this plot shows that we should only be able to detect greater TLNs in bigger BHs due to the inverse relationship mentioned before. For example, a TLN of 0.012 (blue line in Figure 3.6 should be detectable in smaller BHs but not in SMBHs since the value of L_* would be above the Hubble distance.

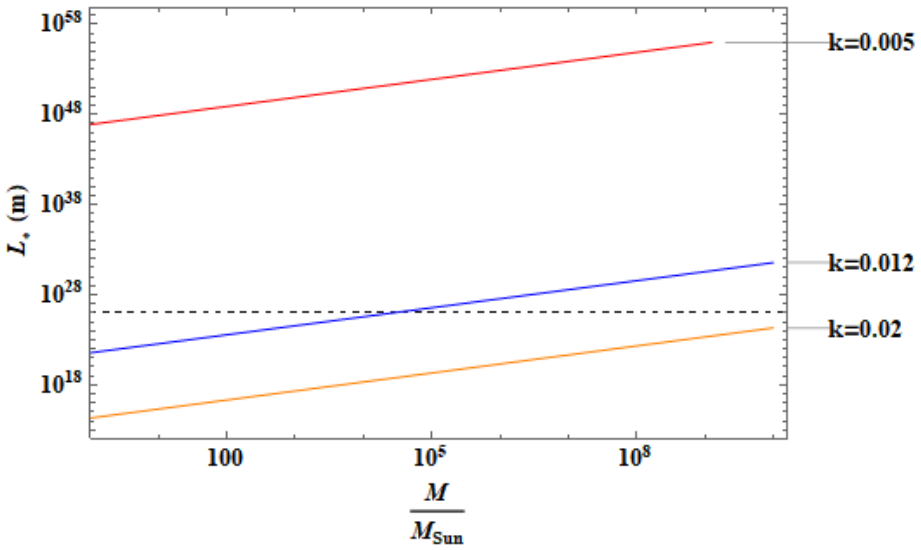

Figure 3.6: Minimum detectable value of L_* for a range of Masses of EUP BHs. Three different values of TLNs have been used. The dashed line represents the Hubble distance of 10^{26}.

CHAPTER 4: CONCLUSIONS

This paper examined black holes' observables under a Schwarzchild EUP-modified metric. These observables could provide a real test for the EUP, and in doing so take a step closer to a theory of Quantum Gravity. We analyzed three different observables and their dependence on the Mass of the black hole and the value of L_*, and in some cases, we were able to compare to Schwarzchild-only results. To do so, we used a similar approach to the one presented in section 2.2. We assumed that the perturbation to the metric would create a near-horizon structure that would produce a reflective surface, and as such produce observable effects that could be measured by near-future technology like LISA or the EHT. Based on this approach, it was shown throughout chapter 3 that the EUP modification does produce significant deviations from the standard solution, especially for higher values of L_*. This behavior was shown for GWs Echoes, QNMs, and TLNs. Future research projects will be able to use the theoretical results shown in this article, to test them against the experimental values found. Additionally, some of the solutions presented in this paper have been approximated for special cases of ϵ, and as such finding the exact solutions would be useful for future analysis.

BIBLIOGRAPHY

[1] S. Chandrasekhar, American Journal of Physics **40**, 224 (1972), https://doi.org/10.1119/1.1986496 .

[2] K. Schwarzschild, Sitzungsber. Preuss. Akad. Wiss. Berlin (Math. Phys.) **1916**, 189 (1916), arXiv:physics/9905030 .

[3] C. Cataldo, International Journal of Advanced Engineering Research and Science **4**, 48 (2017).

[4] K. Martel and E. Poisson, American Journal of Physics **69**, 476 (2001), https://doi.org/10.1119/1.1336836 .

[5] W. Heisenberg, Zeitschrift fÃ¼r Physik **43**, 172 (1927).

[6] M. Ozawa, Current science **109** (2015), 10.18520/cs/v109/i11/2006-2016.

[7] R. J. Adler and D. I. Santiago, Modern Physics Letters A **14**, 1371 (1999).

[8] C. Bambi and F. R. Urban, Classical and Quantum Gravity **25**, 095006 (2008), arXiv: 0709.1965.

[9] B. Bolen and M. Cavagliá, General Relativity and Gravitation **37**, 1255 (2005).

[10] A. Kempf, G. Mangano, and R. B. Mann, Physical Review D **52**, 1108 (1995), arXiv: hep-th/9412167.

[11] J. R. Mureika, Physics Letters B **789**, 88 (2019).

[12] C. Rovelli, Living Reviews in Relativity **11**, 5 (2008).

[13] S. Mukhi, Classical and Quantum Gravity **28**, 153001 (2011).

[14] P. Nicolini, International Journal of Modern Physics A **24**, 1229 (2009), https://doi.org/10.1142/S0217751X09043353 .

[15] The LIGO Scientific Collaboration, https://www.ligo.org/.

[16] The Event Horizon Telescope Collaboration, http://www.eventhorizontelescope.org/.

[17] LIGO Scientific Collaboration and Virgo Collaboration, Phyical Review Letters **116**, 061102 (2016).

[18] The Event Horizon Telescope Collaboration, The Astrophysical Journal Letters **875**, L1 (2019), publisher: The American Astronomical Society.

[19] G. Dvali and C. Gomez, "Black hole's information group," (2013), arXiv:1307.7630 [hep-th] .

[20] L. Buoninfante, G. Lambiase, G. G. Luciano, and L. Petruzziello, The European Physical Journal C **80**, 853 (2020), arXiv: 2001.05825.

[21] V. Cardoso and P. Pani, Living Reviews in Relativity **22**, 4 (2019).

[22] J. Abedi, H. Dykaar, and N. Afshordi, Physical Review D **96** (2017), 10.1103/physrevd.96.082004.

[23] V. Cardoso, S. Hopper, C. F. Macedo, C. Palenzuela, and P. Pani, Physical Review D **94** (2016), 10.1103/physrevd.94.084031.

[24] S. Chandrasekhar and S. Detweiler, Proceedings of the Royal Society of London. A. Mathematical and Physical Sciences **344**, 441 (1975), https://royalsocietypublishing.org/doi/pdf/10.1098/rspa.1975.0112 .

[25] K. D. Kokkotas and B. G. Schmidt, Living Reviews in Relativity **2** (1999), 10.12942/lrr-1999-2, https://www.ncbi.nlm.nih.gov/pmc/articles/PMC5253841/ .

[26] E. Berti, V. Cardoso, and A. O. Starinets, Classical and Quantum Gravity **26**, 163001 (2009).

[27] V. Cardoso, E. Franzin, A. Maselli, P. Pani, and G. Raposo, Physical Review D **95** (2017), 10.1103/physrevd.95.084014.